Title

Individual differences in GABA content are reliable but are not uniform across the human cortex

Authors

Greenhouse, Ian
Noah, Sean
Maddock, Richard J
et al.

Publication Date

2016-10-01

DOI

10.1016/j.neuroimage.2016.06.007

Peer reviewed

Individual differences in GABA content are reliable but are not uniform across the human cortex

Ian Greenhouse*[1], Sean Noah[1], Richard J Maddock[2], Richard B Ivry[1]

1. University of California, Berkeley, Berkeley, California

2. University of California, Davis, Davis, California

***Corresponding Author:** Ian Greenhouse
3201 Tolman Hall
University of California, Berkeley
Berkeley, CA 94720-1650

E-mail: igreenhouse@berkeley.edu
Phone: +1 (510) 642-0135

Abstract

^{1}H magnetic resonance spectroscopy (MRS) provides a powerful tool to measure gamma-aminobutyric acid (GABA), the principle inhibitory neurotransmitter in the human brain. We asked whether individual differences in MRS estimates of GABA are uniform across the cortex or vary between regions. In two sessions, resting GABA concentrations in the lateral prefrontal, sensorimotor, dorsal premotor, and occipital cortices were measured in twenty-eight healthy individuals. GABA estimates within each region were stable across weeks, with low coefficients of variation. Despite this stability, the GABA estimates were not correlated between regions. In contrast, the percentage of brain tissue per volume, a control measure, was correlated between the three anterior regions. These results provide an interesting dissociation between an anatomical measure of individual differences and a neurochemical measure. The different patterns of anatomy and GABA concentrations have implications for understanding regional variation in the molecular topography of the brain in health and disease.

Keywords:

Individual differences; GABA; Magnetic resonance spectroscopy; Cortex; Molecular Topography; Inhibition

Introduction

Immunohistochemical, enzymatic, chromatographic and radioreceptor assays in humans and non-human species have demonstrated that γ-aminobutyric acid (GABA) concentrations vary across brain regions (Baxter, 1970). The initial work on this problem, performed predominantly *ex vivo*, helped establish GABA's role as the primary inhibitory neurotransmitter in the vertebrate brain. Recent studies have focused on the local distribution of GABA receptor subtypes (Watanabe et al., 2002), including genetic contributions to the molecular topography across the entire brain (Hawrylycz et al., 2012). While this work has characterized synaptic GABA mechanisms and suggests that gene transcription is relatively homogenous throughout the neocortex, an open question concerns whether individual differences in GABA levels are uniform throughout the cortex or are region-specific. The answer to this question is important for understanding GABA's role in mediating widespread versus local brain functions.

In vivo ^{1}H magnetic resonance spectroscopy (MRS) measures metabolite concentrations, including GABA, with sufficient sensitivity to detect individual differences. To date, three studies have assayed different regions and reported that GABA levels were not correlated between brain regions (Boy et al., 2010; Grachev and Apkarian, 2000; Grachev et al., 2001). However, these studies did not assess measurement reliability, a prerequisite for investigating individual differences. Consequently, the lack of relationships between brain regions in these studies could arise from inter-regional differences in measurement reliability.

To evaluate the spatial scale at which GABA levels are mediated in the brain, we obtained Mescher-Garwood point-resolved spectroscopy (MEGA-PRESS) measurements

of GABA from the lateral prefrontal (LPF), sensorimotor (SM), dorsal premotor (PMd), and occipital (OCC) cortices. Measurements were made during two separate sessions, approximately two weeks apart, to assess reliability (Bogner et al., 2010; Evans et al., 2010; Geramita et al., 2011; Near et al., 2014; O'Gorman et al., 2011; Stephenson et al., 2011). These measurements were combined across the two sessions and used to compare GABA estimates between regions. As a point of contrast, we compared brain tissue per volume between the same four measurement regions. This measure and a coregistration procedure were used to assess the reliability of voxel positioning across sessions.

Materials and methods

Participants

Twenty-eight males (21.8 ± .4 years of age) were scanned in two sessions (16 ± 3 days apart). All participants provided informed consent following a protocol approved by the IRB of the University of California, Berkeley, and were screened for magnetic resonance imaging contraindications.

Magnetic Resonance Imaging and Spectroscopy Acquisition

MR data were acquired using a 3 Tesla Siemens TIM/trio scanner (Berlin/Munich, Germany) with a 32-channel radiofrequency head coil. Each scanning session consisted of two T1-weighted anatomical scans (sagittal MPRAGE, TR/TE = 1900/2.52ms, 900 ms TI, flip angle = 9°, FoV 250 x 176, 1 mm^3 voxel size, acceleration factor of two) and eight MEGA-PRESS scans (320 transients per scan – 160 Off and 160 On, TR/TE = 1500/68 ms, 1.9 ppm and 7.5 ppm On- and Off-resonance edit pulse frequencies, 45 Hz

88 edit pulse bandwidth, delta frequency of -1.7 ppm relative to water – optimized for signal
89 detection at 3.00 ppm, 50 Hz water suppression bandwidth, TA = 8.4 min). MEGA-
90 PRESS averages were collected in pairs, alternating between On- and Off-resonance
91 editing pulses.

92 MRS data were acquired within each of four voxels, designed to target right
93 lateral prefrontal cortex (LPF; 25 x 40 x 25 mm), right sensorimotor cortex (SM; 30 x 30
94 x 30 mm), right dorsal premotor cortex (PMd; 25 x 40 x 25 mm), and bilateral occipital
95 cortex (OCC; 30 x 30 x 30 mm). Voxel orientations maximized the amount of grey
96 matter relative to white matter and CSF within each voxel, while also accommodating
97 each individual participant's anatomy. The LPF and SM voxels were prescribed in
98 reference to the first T1-weighted scan, and the PMd and OCC voxels were prescribed in
99 reference to the second T1-weighted scan. Thus, the imaging protocol consisted of one
100 T1 weighted scan followed by LPF (x 2) and SM (x 2) acquisitions. A separate T1
101 weighted scan was then acquired, followed by PMd (x 2) and OCC (x 2, if time allowed)
102 MRS acquisitions. Shimming for each voxel involved a combined automated and manual
103 routine that was performed immediately after each voxel was positioned. Each voxel was
104 sampled in two consecutive 8.4-minute scans and the order of scans was consistent across
105 all participants and visits. Maintaining a constant order for all participants controlled for
106 temporal relationships that could influence data acquisition during each scan session.

107 The T1-weighted image was resliced into axial and coronal views, and voxels
108 were positioned relative to anatomical landmarks using all three planar views (Fig. 1A).
109 The outer surfaces of all voxels remained several millimeters inside the brain to allow for
110 imperfect RF profiles for volume selection and editing, a limitation of the MEGA-PRESS

sequence (Kaiser et al., 2008) and ensured that measurements did not extend outside the cortical surface. Gradient orders for each voxel were optimized to reduce artifacts as determined during pilot testing (Ernst and Chang, 1996).

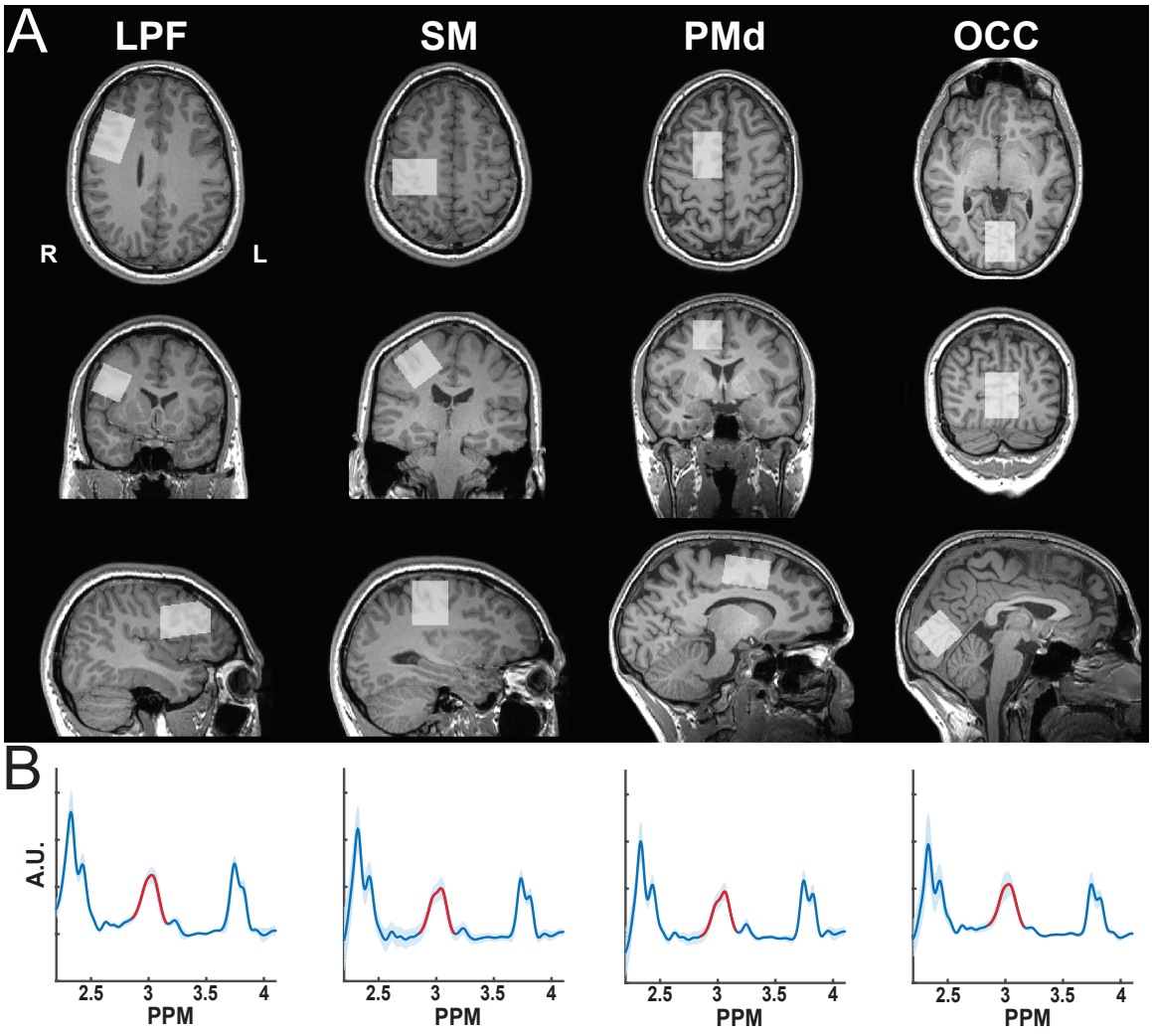

Fig. 1.

Voxel Positioning and GABA Estimation. (A) MRS measurements were made during two scanning sessions from voxels prescribed in the lateral prefrontal (LPF), sensorimotor (SM), dorsal premotor (PMd), and occipital (OCC) cortices. (B) GABA+ signal was quantified by integrating the difference spectra under the peak centered at 3.00 ppm.

The LPF voxel was centered over the inferior frontal junction, with the longest axis extending anterior to posterior. One surface of the LPF voxel followed the outer surface of the cortex in both the coronal and axial views. The SM voxel was centered over the hand knob, parallel to the anterior to posterior axis. One surface of the SM voxel was parallel to the cortical surface in the coronal and axial views. The PMd voxel was positioned with its posterior surface aligned to the precentral sulcus, the lateral surface parallel to the right medial wall of the longitudinal fissure, and the dorsal surface parallel to the cortical surface along the anterior to posterior axis. The OCC voxel was centered bilaterally over the calcarine sulcus extending equally into the left and right hemispheres. The ventral surface of the OCC voxel was parallel to the straight sinus.

Sagittal, axial, and coronal views of each voxel, registered to the T1-weighted image acquired at the first session, were used to guide positioning of each voxel at the second session. First, the center coordinates and orientation for each voxel from the first session were used to initialize the position of each voxel at the second session. To adjust for differences in head position, manual translations and rotations were made using the anatomical landmarks identified during the first session.

Data Analysis

All data were analyzed using customized routines in Matlab (Natick, MA). The scans were exported in Siemens .rda format, with sets of 10 consecutive transients averaged and stored in a single .rda file. This yielded 32 .rda files for each scan (16 On and 16 Off). Preprocessing of the spectra included zero-filling spectra from 1024 to 4096 data points

and apodization with a 4 Hz Gaussian function. Off-resonance spectra were manually phase corrected and aligned with reference to creatine (Cr). Correction values were applied to the paired On-resonance spectra (Evans et al., 2013; Near et al., 2015). The mean and standard deviation were calculated at each frequency of each On- and Off-resonance spectrum, and the number of deviant values (> 2 standard deviations from the mean) was tallied. The spectra were visually inspected to identify those which should be excluded from further analysis based on the number of deviant values and overt corruption or distortion of the spectra (Near et al., 2013; Simpson et al., 2015). The complete analysis code is available for download at https://osf.io/3gsdt/. The mean number of spectra removed was .5 ± .4% for the LPF, .4 ± .3% for the SM, .3 ± .2% for the PMd, and 0% for the OCC voxel. There was no evidence that the quality of data changed within a session or between sessions as assessed by the number of deviant values.

Peak integration was performed using a previously published method (Yoon et al., 2010). In brief, the signal was integrated beneath the GABA+ peak (range: 2.85 to 3.15 ppm, Fig. 1B) in the difference spectra and the Cr peak (range: 2.93 to 3.10 ppm) in the summed On- and Off-resonance spectra. The ratio of total GABA+ to total Cr signal (GABA+/Cr) was calculated from the average preprocessed spectra acquired within each scan. This GABA+/Cr ratio accounts for scanner-related factors that might impact signal-to-noise differently within/between scans or days, and that could differentially impact reference peaks away from 3 ppm (Mullins et al., 2014). Data included in the final analyses were comprised of spectra from two scans (160 measures each) acquired within each session (4 total scans) and screened for artifacts. Participants who provided three or fewer scans were excluded. This conservative approach to data inclusion yielded LPF

data from 20 participants, SM data from 22 participants, PMd data from 24 participants, and OCC data from 15 participants. Due to time constraints in the scanner, and because the OCC voxel was always acquired last, the OCC data were only acquired in a subset of participants at both sessions. We note that the OCC findings are considered exploratory because they were obtained from a smaller sample.

Pearson correlations of GABA+/Cr ratios between sessions were performed to assess reliability across days for each voxel, and coefficients of variation were calculated within participants for each voxel, as an estimate of the signal-to-noise ratio. Using the data averaged across the two sessions, Pearson correlations between pairs of voxels were performed to test whether individual differences in GABA+/Cr ratios in one brain area predicted differences in another brain area. The same comparisons were performed for GABA+ estimates alone to rule out the possibility that Cr estimates might account for any observed relationships. The GABA+ estimates taken on their own are more susceptible to differences in the magnetic field across scans or other scanner related factors, but this analysis helps to constrain interpretations.

The percent total volume of grey matter, white matter, and cerebrospinal fluid (CSF) were calculated within each voxel using the FMRIB's Automated Segmentation Tool (Zhang et al., 2001; http://fsl.fmrib.ox.ac.uk/). The percent tissue relative to total voxel volume ([grey matter + white matter]/total volume) was first used to compare the reliability of voxel placement between the two scans. Agreement between scans is unlikely to be accounted for by artifacts that are specific to a single scan, such as head motion. These same measures were used to compare percent tissue between voxels. We note that while head motion might globally affect T1-weighted images, we used one T1-

weighted image to calculate tissue percentages for the PMd and OCC voxels and a separate T1-weighted image to calculate tissue percentages for the LPF and SM voxels at each session. This approach controlled for motion artifacts that could introduce artificial relationships in tissue estimates across regions that would be expected for an image derived from a single scan.

To further assess the reliability of voxel placement between visits, we coregistered the T1-weighted images from the second visit to those acquired at the first visit using the FMRIB FLIRT registration toolbox (rigid-body coregistration with six degrees of freedom). The resulting registration matrices were applied to three-dimensional reconstructed masks of the MRS voxels acquired at the second visit, with reference to the appropriate T1-weighted images. After coregistration, we calculated the percent overlap of each pair of voxels between visits (e.g., the LPF voxel at visit 1 relative to the LPF voxel at visit 2) using the fslmaths tools.

Total tissue percentage, percent GM, and percent WM for each voxel were correlated with the metabolite estimates to test for relationships between GABA+/Cr and tissue subtypes. Coefficients of variation (CVs) were used to assess the relative variability of measurements across sessions, with lower values reflecting greater reliability.

Results

Percent brain tissue is reliable but not correlated with GABA+/Cr ratios

Tissue percentages within each voxel were highly correlated across sessions (LPF: $r = .82$, $p < .001$, SM: $r = .89$, $p < .001$, PMd: $r = .82$, $p < .001$, OCC: $r = .82$, $p < .001$;

Fig. 2A) and exhibited low CVs (Table S1). A similar pattern was observed for percent GM and percent WM (Fig. S1, S2, & Table S1). Averaged across sessions, percent total tissue was 91 ± .03%, 90 ± .04%, 91 ± .03%, and 90 ± .04% for the LPF, SM, PMd, and OCC voxels, respectively. The coregistration procedure showed that there was 90.6 ± 1.4% overlap between sessions for the LPF voxels, 90.5 ± 1.9% overlap for the SM voxel, 90.9 ± 2.0% overlap for the PMd voxel, and 89.8 ± 2.5% overlap for the OCC voxel. We note that the automated coregistration method may introduce some error.

GABA+/Cr ratios were not correlated with tissue percentages (Fig. 2B), percent GM (Fig. S3), or percent WM (Fig. S4) within any voxel. For this reason, and because we did not estimate absolute concentrations (Kreis et al., 1993a; 1993b), we did not "correct" our GABA+/Cr estimates as a function of tissue volume estimates, e.g. (Harris et al., 2015). Furthermore, we did not observe any relationships between tissue composition and GABA+ or Cr estimates alone for any of our voxels (GM and GABA+: all voxels $p > .13$, Fig. S5; WM and GABA+: all voxels $p > .14$, Fig. S6; GM and Cr: all voxels $p > .27$, Fig. S7; WM and Cr: all voxels $p > .11$, Fig. S8).

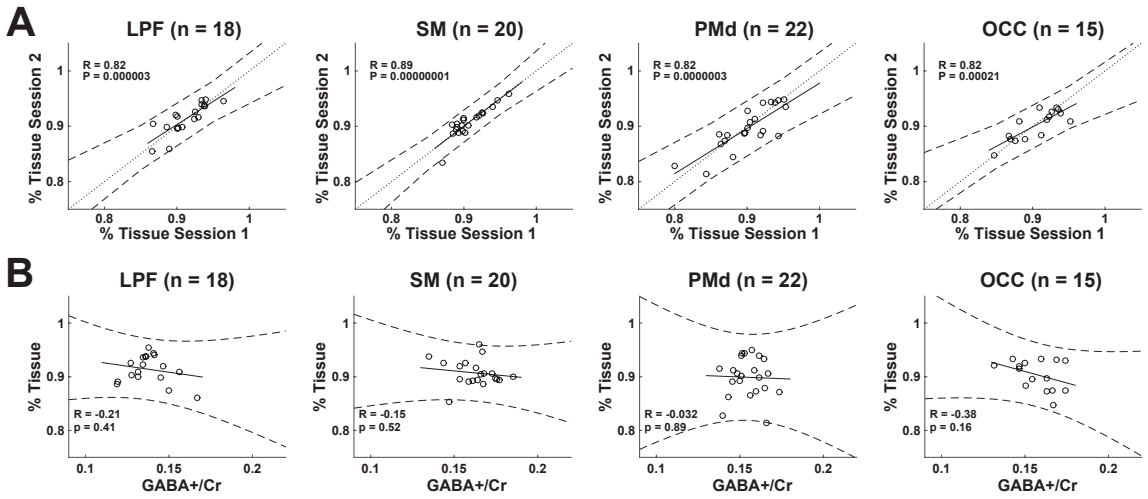

Fig. 2.

Reliability of Voxel Positioning and Percent Tissue Correlation with GABA+/Cr. (A) Tissue density within the lateral prefrontal (LPF), sensorimotor (SM), dorsal premotor (PMd), and occipital (OCC) voxels were highly reliable across sessions in all four voxels. (B) Using average measures across sessions, percent tissue per volume did not predict GABA+/Cr ratios.

GABA+/Cr ratios and GABA+ alone are reliable within sessions and across weeks

The GABA+/Cr ratios were reliable between the two scans within each session (LPF: R = .75, $p < .001$, CV = 4.6 ± 0.9%; SM: R = .64, $p < .01$, CV = 3.9 ± 1.0%; PMd: R = .63, $p < .005$, CV = 3.9 ± 0.7%; OCC: R = .52, $p < .05$, CV = 5.3 ± 1.1%). GABA+/Cr ratios were also stable across weeks in all four voxels (Fig. 3A). The CVs were 5.9 ± .93% (range .7–16.1%) for LPF, 5.3 ± .98% (range .2–16.9%) for SM, 3.8 ± .60% (range .04–11.6%) for PMd, and 5.3 ± .92% (range .73–16.0%) for OCC voxels. These values are in agreement with previous studies (Evans et al., 2010; Near et al., 2014; Stephenson et al., 2011; Wijtenburg et al., 2013). Estimates of GABA+ alone, expressed in arbitrary units, exhibited a similar pattern of reliability, although the correlation in OCC only reached

trend-level significance (LPF: r = .46, p < .05, SM: r = .7, p < .001, PMd: r = .56, p < .005, OCC: r = .49, p = .06; Fig. 3B).

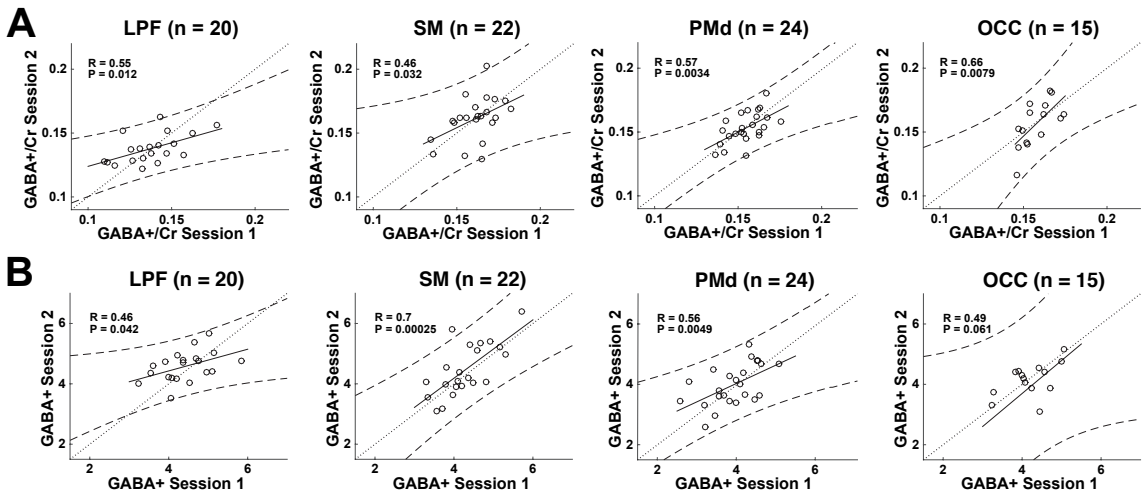

Fig. 3.

GABA+/Cr Ratios and Raw GABA+ Estimates were Reliable. (A) GABA+/Cr ratios were reliable across sessions within the lateral prefrontal (LPF), sensorimotor (SM), dorsal premotor (PMd), and occipital (OCC) voxels. (B) GABA+ estimates were also reliable across sessions, indicating that scanning related factors were consistent between days and that Cr alone is unlikely to account for the reliable GABA+/Cr ratios.

GABA+/Cr and tissue comparisons across brain regions

The preceding analyses indicate that MR scanner performance and MRS voxel positioning were consistent across the two sessions. Moreover, the observed reliability for the GABA+/Cr ratios cannot be explained by Cr measurements alone. This allowed us to turn to our main question: whether individual differences in intrinsic GABA are consistent between cortical regions.

We averaged the GABA+/Cr ratios across the two sessions and tested for correlations between each pair of voxels. Importantly, individual differences in GABA+/Cr within one voxel did not predict individual differences at the other voxels (all p's > .06, Fig. 4A). This result suggests that intrinsic cortical GABA+ content is determined locally. The correlation approached significance for the PMd and SM voxels (p = .06), although it is important to keep in mind that, because of their proximity, these two voxels overlapped by approximately 5% of their total volume (11.2 ± 5.3 mm^3).

In contrast to GABA+/Cr, total tissue percentages were correlated between the LPF, SM, and PMd voxels (all p's < .05 uncorrected, Fig. 4B), with only the correlation between the SM and PMd voxels surviving a more stringent multiple comparison correction (p < .0125). Thus, individual differences in total tissue percentages were consistent between the anterior voxels.

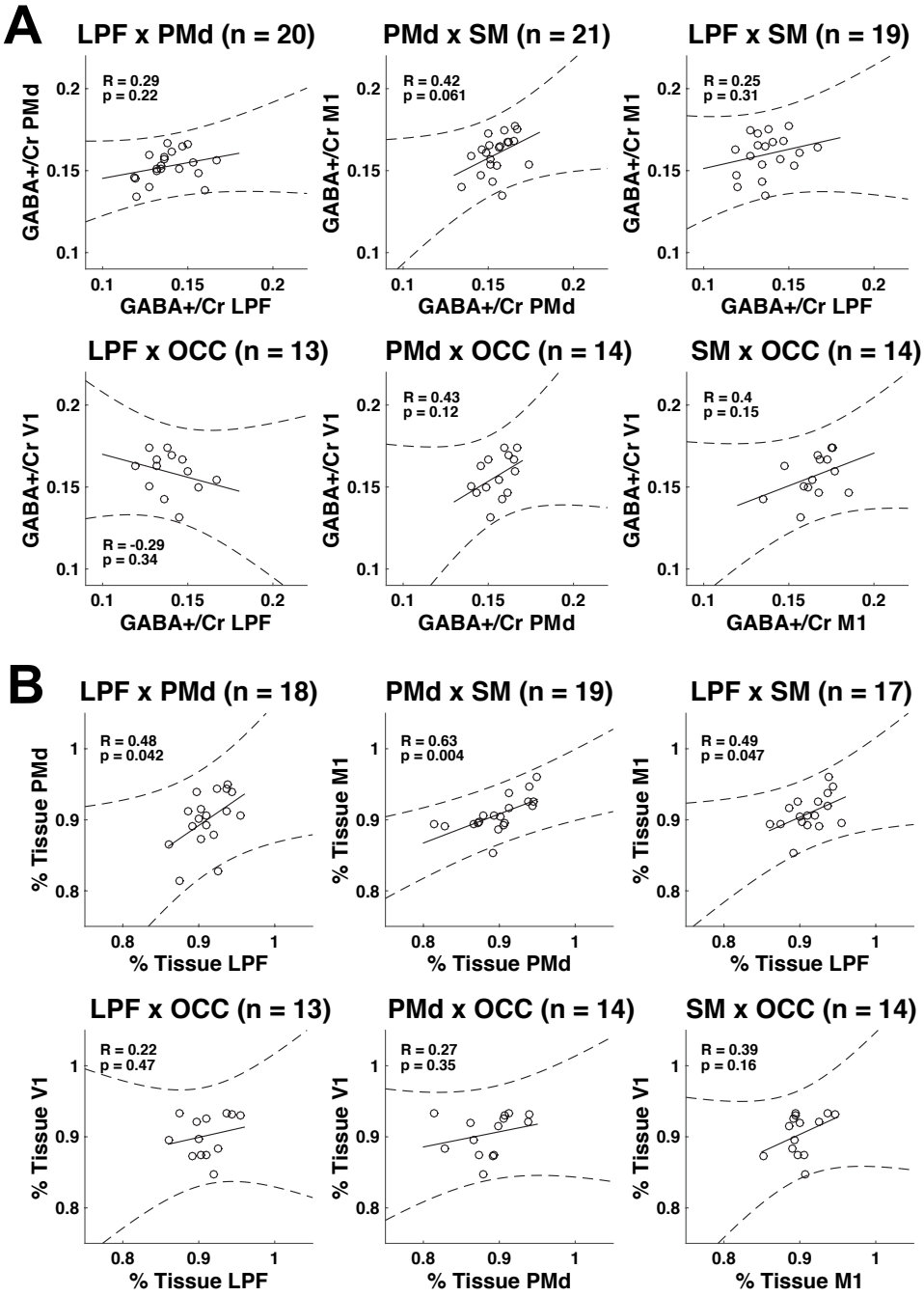

Fig. 4.

Tissue Density but not GABA+/Cr is Correlated Between Voxels. (A) GABA+/Cr ratios were not significantly correlated in any pairwise comparison of the four voxels. (B) Tissue density was correlated between the lateral prefrontal (LPF), sensorimotor (SM), and dorsal premotor (PMd) voxels, but these frontal regions were not correlated with the occipital (OCC) voxel.

Discussion

The study of individual differences is essential for understanding behavioral and biological variation. In the neurosciences, this approach lends insight into biomarkers of brain function and gene-environment interactions. A recurring question concerns the regional specificity versus uniformity of individual differences throughout the brain. For example, recent evidence suggests that a relatively homogenous 'transcriptional blueprint' exists throughout the cortex (Hawrylycz et al., 2012; Richiardi et al., 2015). Epigenetic factors demonstrate homogeneity across brain regions as well. Specifically, DNA methylation is more similar across different brain regions within an individual than for a single brain region compared across individuals (Illingworth et al., 2015). Moreover, individual differences in white matter integrity (Penke et al., 2010) and diffusivity (Johnson et al., 2015), as well as gray matter density (Mechelli et al., 2005), are relatively uniform throughout the brain. All of these general factors could influence neurotransmitter concentrations. Indeed, local tissue percentages and tissue types have previously been linked to brain metabolite concentrations, including GABA (Bergmann et al., 2015; Harris et al., 2015; Jensen et al., 2005; Kreis et al., 1993b; 1993a).

Given these considerations it is surprising that individual differences in GABA+/Cr ratios were not correlated between neighboring cortical regions. These results are consistent with previous assessments of regional variation in GABA (Boy et al., 2010; Grachev and Apkarian, 2000) and provide two important advances. First, we performed comparisons between regions after establishing measurement reliability across two sessions, a prerequisite for studying individual differences. Notably, intra-voxel reliability was assessed between sessions, whereas comparisons between regions included

317 data acquired within sessions. Our conclusions are thus conservative in that inter-session
318 variability should impact reliability estimates to a greater degree than between-region
319 comparisons. Second, the local variation in intrinsic GABA stands in contrast to a
320 structural measure: The percentage of brain tissue, within the same voxels, was correlated
321 between anterior cortical regions. Taken together, these measures suggest that anatomical
322 and neurochemical individual differences occur at different spatial scales in the cortex.

323 Previous MRS studies reported correlations between behavioral or
324 neurophysiological measures and GABA estimates within targeted brain regions
325 (Bachtiar et al., 2015; Balz et al., 2016; Boy et al., 2010; Heba et al., 2016; Jocham et al.,
326 2012; Stagg et al., 2011a; 2011b; Sumner et al., 2010; van Loon et al., 2013). For
327 example, resting GABA content in primary motor cortex was positively correlated with
328 individual differences in motor sequence reaction time (Stagg et al., 2011a). Our results
329 are consistent with the hypothesis that locally determined neurotransmitter content relates
330 to the functional specialization of brain regions. Moreover, the finding that resting GABA
331 measurements within multiple cortical regions remained relatively stable across weeks
332 suggests that task-dependent changes in GABA (Floyer-Lea et al., 2006; Michels et al.,
333 2012) likely occur on top of stable basal levels.

334 Our results have important clinical implications. Abnormalities in GABA
335 concentrations have been associated with neurological diseases and trauma (Blicher et al.,
336 2015; Dharmadhikari et al., 2015; Draper et al., 2014; Hattingen et al., 2014; van der Hel
337 et al., 2013). Given the reliability observed here in healthy individuals, it may be possible
338 to relate local changes in GABA to patterns of recovery. Similarly, one could assess the

anatomical specificity of medications that impact GABA-dependent processes, e.g. benzodiazepines or selective serotonin reuptake inhibitors (Bhagwagar et al., 2004).

The MRS method applied here measures metabolite concentrations throughout the entire voxel, including perivesicular and cytoplasmic environments. While we did not observe inter-regional correlations in GABA measurements, it is possible that specific compartments, e.g. vesicular or synaptic GABA, are similar across brain regions. Furthermore, we only studied young adult males. Our results may not translate to females or to older populations, as GABA content has been found to differ between the sexes (Epperson et al., 2002; O'Gorman et al., 2011) and to decrease with age (Gao et al., 2013). In addition, the GABA+ signal at 3.00 ppm includes contributions from coedited macromolecules as well as homocarnosine, a GABA derivative; indeed, this is a principle limitation of the method. We did not control for macromolecules in our data, and the effects we observed could include a macromolecular contribution. It is also possible that differences in creatine content between regions influenced our results.

In summary, measurements of GABA+/Cr obtained across weeks exhibited marked reliability, but had little shared variance across brain regions. Thus, while individual differences in cortical GABA concentrations are stable, variation in these concentrations is locally determined. These results support the use of MRS for assessing local neurotransmitter concentrations, with potential clinical utility for assessing sensitivity to treatment interventions or monitoring disease progression.

Acknowledgements

This work was supported by NIH grant NS085570. We thank Jamie Near for sharing analysis code.

References

Bachtiar, V., Near, J., Johansen-Berg, H., Stagg, C.J., 2015. Modulation of GABA and resting state functional connectivity by transcranial direct current stimulation. Elife 4, 1023. doi:10.7554/eLife.08789

Balz, J., Keil, J., Roa Romero, Y., Mekle, R., Schubert, F., Aydin, S., Ittermann, B., Gallinat, J., Senkowski, D., 2016. GABA concentration in superior temporal sulcus predicts gamma power and perception in the sound-induced flash illusion. NeuroImage 125, 724–730. doi:10.1016/j.neuroimage.2015.10.087

Baxter, C.F., 1970. The Nature of γ-Aminobutyric Acid, in: Metabolic Reactions in the Nervous System. Springer US, Boston, MA, pp. 289–353. doi:10.1007/978-1-4615-7160-5_9

Bergmann, J., Pilatus, U., Genç, E., Kohler, A., Singer, W., Pearson, J., 2015. V1 surface size predicts GABA concentration in medial occipital cortex. NeuroImage 124, 654–662. doi:10.1016/j.neuroimage.2015.09.036

Bhagwagar, Z., Wylezinska, M., Taylor, M., Jezzard, P., Matthews, P.M., Cowen, P.J., 2004. Increased brain GABA concentrations following acute administration of a selective serotonin reuptake inhibitor. Am J Psychiatry 161, 368–370. doi:10.1176/appi.ajp.161.2.368

Blicher, J.U., Near, J., Næss-Schmidt, E., Stagg, C.J., Johansen-Berg, H., Nielsen, J.F., Østergaard, L., Ho, Y.-C.L., 2015. GABA levels are decreased after stroke and GABA changes during rehabilitation correlate with motor improvement. Neurorehabilitation and Neural Repair 29, 278–286. doi:10.1177/1545968314543652

Bogner, W., Gruber, S., Doelken, M., Stadlbauer, A., Ganslandt, O., Boettcher, U.,

391 Trattnig, S., Doerfler, A., Stefan, H., Hammen, T., 2010. In vivo quantification of
392 intracerebral GABA by single-voxel (1)H-MRS-How reproducible are the results?
393 Eur J Radiol 73, 526–531. doi:10.1016/j.ejrad.2009.01.014
394 Boy, F., Evans, C.J., Edden, R.A.E., Singh, K.D., Husain, M., Sumner, P., 2010.
395 Individual differences in subconscious motor control predicted by GABA
396 concentration in SMA. Curr Biol 20, 1779–1785. doi:10.1016/j.cub.2010.09.003
397 Dharmadhikari, S., Ma, R., Yeh, C.-L., Stock, A.-K., Snyder, S., Zauber, S.E., Dydak, U.,
398 Beste, C., 2015. Striatal and thalamic GABA level concentrations play differential
399 roles for the modulation of response selection processes by proprioceptive
400 information. NeuroImage 120, 36–42. doi:10.1016/j.neuroimage.2015.06.066
401 Draper, A., Stephenson, M.C., Jackson, G.M., Pépés, S., Morgan, P.S., Morris, P.G.,
402 Jackson, S.R., 2014. Increased GABA contributes to enhanced control over motor
403 excitability in Tourette syndrome. Curr Biol 24, 2343–2347.
404 doi:10.1016/j.cub.2014.08.038
405 Epperson, C.N., Haga, K., Mason, G.F., Sellers, E., Gueorguieva, R., Zhang, W., Weiss,
406 E., Rothman, D.L., Krystal, J.H., 2002. Cortical gamma-aminobutyric acid levels
407 across the menstrual cycle in healthy women and those with premenstrual dysphoric
408 disorder: a proton magnetic resonance spectroscopy study. Arch Gen Psychiatry 59,
409 851–858.
410 Ernst, T., Chang, L., 1996. Elimination of artifacts in short echo time H MR spectroscopy
411 of the frontal lobe. Magn Reson Med 36, 462–468.
412 Evans, C.J., McGonigle, D.J., Edden, R.A.E., 2010. Diurnal stability of gamma-
413 aminobutyric acid concentration in visual and sensorimotor cortex. J Magn Reson

414 Imaging 31, 204–209. doi:10.1002/jmri.21996
415 Evans, C.J., Puts, N.A.J., Robson, S.E., Boy, F., McGonigle, D.J., Sumner, P., Singh,
416 K.D., Edden, R.A.E., 2013. Subtraction artifacts and frequency (mis-)alignment in J-
417 difference GABA editing. J Magn Reson Imaging 38, 970–975.
418 doi:10.1002/jmri.23923
419 Floyer-Lea, A., Wylezinska, M., Kincses, T., Matthews, P.M., 2006. Rapid modulation of
420 GABA concentration in human sensorimotor cortex during motor learning. Journal of
421 Neurophysiology 95, 1639–1644. doi:10.1152/jn.00346.2005
422 Gao, F., Edden, R.A.E., Li, M., Puts, N.A.J., Wang, G., Liu, C., Zhao, B., Wang, H., Bai,
423 X., Zhao, C., Wang, X., Barker, P.B., 2013. Edited magnetic resonance spectroscopy
424 detects an age-related decline in brain GABA levels. NeuroImage 78, 75–82.
425 doi:10.1016/j.neuroimage.2013.04.012
426 Geramita, M., van der Veen, J.W., Barnett, A.S., Savostyanova, A.A., Shen, J.,
427 Weinberger, D.R., Marenco, S., 2011. Reproducibility of prefrontal γ-aminobutyric
428 acid measurements with J-edited spectroscopy. NMR Biomed 24, 1089–1098.
429 doi:10.1002/nbm.1662
430 Grachev, I.D., Apkarian, A.V., 2000. Chemical Heterogeneity of the Living Human
431 Brain: A Proton MR Spectroscopy Study on the Effects of Sex, Age, and Brain
432 Region. NeuroImage 11, 554–563. doi:10.1006/nimg.2000.0557
433 Grachev, I.D., Swarnkar, A., Szeverenyi, N.M., Ramachandran, T.S., Apkarian, A.V.,
434 2001. Aging alters the multichemical networking profile of the human brain: an in
435 vivo (1)H-MRS study of young versus middle-aged subjects. J. Neurochem. 77, 292–
436 303.

Harris, A.D., Puts, N.A.J., Edden, R.A.E., 2015. Tissue correction for GABA-edited MRS: Considerations of voxel composition, tissue segmentation, and tissue relaxations. J Magn Reson Imaging 42, 1431–1440. doi:10.1002/jmri.24903

Hattingen, E., Lückerath, C., Pellikan, S., Vronski, D., Roth, C., Knake, S., Kieslich, M., Pilatus, U., 2014. Frontal and thalamic changes of GABA concentration indicate dysfunction of thalamofrontal networks in juvenile myoclonic epilepsy. Epilepsia 55, 1030–1037. doi:10.1111/epi.12656

Hawrylycz, M.J., Lein, E.S., Guillozet-Bongaarts, A.L., Shen, E.H., Ng, L., Miller, J.A., van de Lagemaat, L.N., Smith, K.A., Ebbert, A., Riley, Z.L., Abajian, C., Beckmann, C.F., Bernard, A., Bertagnolli, D., Boe, A.F., Cartagena, P.M., Chakravarty, M.M., Chapin, M., Chong, J., Dalley, R.A., Daly, B.D., Dang, C., Datta, S., Dee, N., Dolbeare, T.A., Faber, V., Feng, D., Fowler, D.R., Goldy, J., Gregor, B.W., Haradon, Z., Haynor, D.R., Hohmann, J.G., Horvath, S., Howard, R.E., Jeromin, A., Jochim, J.M., Kinnunen, M., Lau, C., Lazarz, E.T., Lee, C., Lemon, T.A., Li, L., Li, Y., Morris, J.A., Overly, C.C., Parker, P.D., Parry, S.E., Reding, M., Royall, J.J., Schulkin, J., Sequeira, P.A., Slaughterbeck, C.R., Smith, S.C., Sodt, A.J., Sunkin, S.M., Swanson, B.E., Vawter, M.P., Williams, D., Wohnoutka, P., Zielke, H.R., Geschwind, D.H., Hof, P.R., Smith, S.M., Koch, C., Grant, S.G.N., Jones, A.R., 2012. An anatomically comprehensive atlas of the adult human brain transcriptome. Nature 489, 391–399. doi:10.1038/nature11405

Heba, S., Puts, N.A.J., Kalisch, T., Glaubitz, B., Haag, L.M., Lenz, M., Dinse, H.R., Edden, R.A.E., Tegenthoff, M., Schmidt-Wilcke, T., 2016. Local GABA Concentration Predicts Perceptual Improvements After Repetitive Sensory

460 Stimulation in Humans. Cereb Cortex 26, 1295–1301. doi:10.1093/cercor/bhv296
461 Illingworth, R.S., Gruenewald-Schneider, U., De Sousa, D., Webb, S., Merusi, C., Kerr,
462 A.R.W., James, K.D., Smith, C., Walker, R., Andrews, R., Bird, A.P., 2015. Inter-
463 individual variability contrasts with regional homogeneity in the human brain DNA
464 methylome. Nucleic Acids Res. 43, 732–744. doi:10.1093/nar/gku1305
465 Jensen, J.E., deB Frederick, B., Renshaw, P.F., 2005. Grey and white matter GABA level
466 differences in the human brain using two□dimensional, J□resolved spectroscopic
467 imaging. NMR Biomed 18, 570–576. doi:10.1002/nbm.994
468 Jocham, G., Hunt, L.T., Near, J., Behrens, T.E.J., 2012. A mechanism for value-guided
469 choice based on the excitation-inhibition balance in prefrontal cortex. Nat Neurosci
470 15, 960–961. doi:10.1038/nn.3140
471 Johnson, M.A., Diaz, M.T., Madden, D.J., 2015. Global versus tract-specific components
472 of cerebral white matter integrity: relation to adult age and perceptual-motor speed.
473 Brain Struct Funct 220, 2705–2720. doi:10.1007/s00429-014-0822-9
474 Kaiser, L.G., Young, K., Meyerhoff, D.J., Mueller, S.G., Matson, G.B., 2008. A detailed
475 analysis of localized J-difference GABA editing: theoretical and experimental study
476 at 4 T. NMR Biomed 21, 22–32. doi:10.1002/nbm.1150
477 Kreis, R., Ernst, T., Ross, B.D., 1993a. Development of the human brain: in vivo
478 quantification of metabolite and water content with proton magnetic resonance
479 spectroscopy. Magn Reson Med 30, 424–437.
480 Kreis, R., Ernst, T., Ross, B.D., 1993b. Absolute Quantitation of Water and Metabolites
481 in the Human Brain. II. Metabolite Concentrations. Journal of Magnetic Resonance,
482 Series B 102, 9–19. doi:10.1006/jmrb.1993.1056

Mechelli, A., Friston, K.J., Frackowiak, R.S., Price, C.J., 2005. Structural covariance in the human cortex. J Neurosci 25, 8303–8310. doi:10.1523/JNEUROSCI.0357-05.2005

Michels, L., Martin, E., Klaver, P., Edden, R., Zelaya, F., Lythgoe, D.J., Lüchinger, R., Brandeis, D., O'Gorman, R.L., 2012. Frontal GABA levels change during working memory. PLoS ONE 7, e31933. doi:10.1371/journal.pone.0031933

Mullins, P.G., McGonigle, D.J., O'Gorman, R.L., Puts, N.A.J., Vidyasagar, R., Evans, C.J., Cardiff Symposium on MRS of GABA, Edden, R.A.E., 2014. Current practice in the use of MEGA-PRESS spectroscopy for the detection of GABA. NeuroImage 86, 43–52. doi:10.1016/j.neuroimage.2012.12.004

Near, J., Edden, R., Evans, C.J., Paquin, R., Harris, A., Jezzard, P., 2015. Frequency and phase drift correction of magnetic resonance spectroscopy data by spectral registration in the time domain. Magn Reson Med 73, 44–50. doi:10.1002/mrm.25094

Near, J., Evans, C.J., Puts, N.A.J., Barker, P.B., Edden, R.A.E., 2013. J-difference editing of gamma-aminobutyric acid (GABA): Simulated and experimental multiplet patterns. Magn Reson Med 70, 1183–1191. doi:10.1002/mrm.24572

Near, J., Ho, Y.-C.L., Sandberg, K., Kumaragamage, C., Blicher, J.U., 2014. Long-term reproducibility of GABA magnetic resonance spectroscopy. NeuroImage 99, 191–196. doi:10.1016/j.neuroimage.2014.05.059

O'Gorman, R.L., Michels, L., Edden, R.A., Murdoch, J.B., Martin, E., 2011. In vivo detection of GABA and glutamate with MEGA-PRESS: reproducibility and gender effects. J Magn Reson Imaging 33, 1262–1267. doi:10.1002/jmri.22520

506 Penke, L., Maniega, S.M., Murray, C., Gow, A.J., Hernández, M.C.V., Clayden, J.D.,
507 Starr, J.M., Wardlaw, J.M., Bastin, M.E., Deary, I.J., 2010. A General Factor of
508 Brain White Matter Integrity Predicts Information Processing Speed in Healthy Older
509 People. J Neurosci 30, 7569–7574. doi:10.1523/JNEUROSCI.1553-10.2010
510 Richiardi, J., Altmann, A., Milazzo, A.-C., Chang, C., Chakravarty, M.M., Banaschewski,
511 T., Barker, G.J., Bokde, A.L.W., Bromberg, U., Büchel, C., Conrod, P., Fauth-Bühler,
512 M., Flor, H., Frouin, V., Gallinat, J., Garavan, H., Gowland, P., Heinz, A., Lemaître,
513 H., Mann, K.F., Martinot, J.-L., Nees, F., Paus, T., Pausova, Z., Rietschel, M.,
514 Robbins, T.W., Smolka, M.N., Spanagel, R., Ströhle, A., Schumann, G., Hawrylycz,
515 M., Poline, J.-B., Greicius, M.D., IMAGEN consortium, 2015. BRAIN NETWORKS.
516 Correlated gene expression supports synchronous activity in brain networks. Science
517 348, 1241–1244. doi:10.1126/science.1255905
518 Simpson, R., Devenyi, G.A., Jezzard, P., Hennessy, T.J., Near, J., 2015. Advanced
519 processing and simulation of MRS data using the FID appliance (FID-A)-An open
520 source, MATLAB-based toolkit. Magn Reson Med. doi:10.1002/mrm.26091
521 Stagg, C.J., Bachtiar, V., Johansen-Berg, H., 2011a. The role of GABA in human motor
522 learning. Curr Biol 21, 480–484. doi:10.1016/j.cub.2011.01.069
523 Stagg, C.J., Bestmann, S., Constantinescu, A.O., Moreno, L.M., Allman, C., Mekle, R.,
524 Woolrich, M., Near, J., Johansen-Berg, H., Rothwell, J.C., 2011b. Relationship
525 between physiological measures of excitability and levels of glutamate and GABA in
526 the human motor cortex. The Journal of Physiology 589, 5845–5855.
527 doi:10.1113/jphysiol.2011.216978
528 Stephenson, M.C., Gunner, F., Napolitano, A., Greenhaff, P.L., Macdonald, I.A., Saeed,

N., Vennart, W., Francis, S.T., Morris, P.G., 2011. Applications of multi-nuclear magnetic resonance spectroscopy at 7T. World J Radiol 3, 105–113. doi:10.4329/wjr.v3.i4.105

Sumner, P., Edden, R.A.E., Bompas, A., Evans, C.J., Singh, K.D., 2010. More GABA, less distraction: a neurochemical predictor of motor decision speed. Nat Neurosci 13, 825–827. doi:10.1038/nn.2559

van der Hel, W.S., van Eijsden, P., Bos, I.W.M., de Graaf, R.A., Behar, K.L., van Nieuwenhuizen, O., de Graan, P.N.E., Braun, K.P.J., 2013. In vivo MRS and histochemistry of status epilepticus-induced hippocampal pathology in a juvenile model of temporal lobe epilepsy. NMR Biomed 26, 132–140. doi:10.1002/nbm.2828

van Loon, A.M., Knapen, T., Scholte, H.S., St John-Saaltink, E., Donner, T.H., Lamme, V.A.F., 2013. GABA shapes the dynamics of bistable perception. Curr Biol 23, 823–827. doi:10.1016/j.cub.2013.03.067

Watanabe, M., Maemura, K., Kanbara, K., Tamayama, T., Hayasaki, H., 2002. GABA and GABA receptors in the central nervous system and other organs. Int. Rev. Cytol. 213, 1–47.

Wijtenburg, S.A., Rowland, L.M., Edden, R.A.E., Barker, P.B., 2013. Reproducibility of brain spectroscopy at 7T using conventional localization and spectral editing techniques. J Magn Reson Imaging 38, 460–467. doi:10.1002/jmri.23997

Yoon, J.H., Maddock, R.J., Rokem, A., Silver, M.A., Minzenberg, M.J., Ragland, J.D., Carter, C.S., 2010. GABA Concentration Is Reduced in Visual Cortex in Schizophrenia and Correlates with Orientation-Specific Surround Suppression. J Neurosci 30, 3777–3781. doi:10.1523/JNEUROSCI.6158-09.2010

552 Zhang, Y., Brady, M., Smith, S., 2001. Segmentation of brain MR images through a
553 hidden Markov random field model and the expectation-maximization algorithm.
554 IEEE transactions on medical imaging 20, 45–57. doi:10.1109/42.906424
555